Effect of shape and size of nanofillers on the viscoelasticity of polymer nanocomposites

Dandan Luo [a,b], Haoyu Wu [a,b], Haoxiang Li [a,b], Wenfeng Zhang [a,b], Liqun Zhang [a,b], Yangyang Gao [a,b,*]

[a] Key Laboratory of Beijing City on Preparation and Processing of Novel Polymer Materials, Beijing University of Chemical Technology, 10029, People's Republic of China
[b] State Key Laboratory of Organic-Inorganic Composites, Beijing University of Chemical Technology, 10029, People's Republic of China

ABSTRACT

Polymer nanocomposites (PNCs) are now widely used in various fields. It is modified by adding fillers to improve its various properties during processing and application. In this work, we investigated the viscoelasticity of PNCs respectively filled with nanoparticles, nanorods and nanosheets and compared the effects of filler shape and filler size. It is found that the nanorod has the most outstanding ability to increase the modulus of PNCs among the three, followed by the nanosheet. The increase of filler size can increase the modulus of the system and has little effect on Payne effect. The source of modulus enhancement of PNCs respectively filled with nanorods and nanosheets changes with increasing volume fraction from Rouse dynamics of the polymer chains to the binding force of the filler on the polymer chains and eventually to the filler network. Increasing the filler size makes the Rouse dynamics region and chain confinement region narrower and the permeation threshold lower. However, the source of modulus enhancement of PNCs filled with nanoparticles is mainly the Rouse dynamics of polymer chains, which only conforms to the above mechanism at a high interface degree of nanoparticles.

1. Introduction

The incorporation of different fillers can significantly improve the mechanical properties [1–4], thermal properties [5–9], flame retardant and fire resistance [10–12], magnetic properties [13–15], electrical properties [16–19], dielectric properties [20] and barrier properties [21, 22] of polymer nanocomposites (PNCs). The shape and size [23–26], amount and dispersion, distribution [10,21,27,28], orientation [29,30] of nanofillers may affect the material properties of PNCs, as well as the interaction between fillers and polymers [31–33]. Fillers can also be modified [34,35] to improve their dispersion or enhance their interaction with polymers, and then added to the matrix to enhance the properties of the composite.

From the aspect of material processing process, it is required that the material has suitable viscous and elastic properties. For example, in powder injection molding process, the filler size and shape are important influencing factors for material processing [26,36], and when the filler amount is high, the viscosity of the composite is more sensitive to small changes in the filler properties; the higher filling density and lower mixing viscosity possessed by the spherical filler can well improve the material properties for injection molding process [37]. After the filler enters the polymer matrix, it hinders the flow of the altered continuous phase and restricts the movement of the polymer chains [38,39]. It is therefore easy to see that when nanofillers are added, additional geometrical constraints are added to the polymer chains, which changes the viscosity and elasticity of the composite [40], and the viscoelastic mechanism of the PNCs is immediately altered. It was shown that the energy storage modulus (G′) and the loss modulus (G″) of the PNCs increase significantly after the addition of the filler [36,41,42], with the energy storage modulus indicating the elasticity of the system, while the increase in the loss modulus can be attributed to the presence of more energy dissipation processes after the increase in filler amount. And the higher the amount of the filler, the shorter the linear viscoelastic region of the PNCs [38,40,43]. Much research has been conducted on the theory of mechanical enhancement of PNCs. Li et al. [44], investigated the effect of adding five shapes of fillers to polyethylene on the properties of the composites. The results show that the surface area to volume ratio of the filler can influence the interaction between the filler and the polymer, playing a dominant role in the structure, dynamics and adhesion of the material. Zhao et al. [45], investigated the effect of three different silica fillers on the properties of PNCs, and the results showed that the shape and connectivity of the fillers play an important role in the mechanical enhancement of PNCs. Cui et al. [46], investigated the modulus enhancement mechanism in the glassy and rubbery states. The

results show that the number of contacts between polymer segments and fillers and the degree of chain stretching in the glassy state affect the modulus; while the modulus magnitude in the rubbery state depends on the total surface area of the fillers. Gao et al. [47], investigated the mechanism of interaction of different fillers on polymers at the interface. It was found that different shapes of fillers exert different forms of force on the polymer and that the mobility of the polymer at the interface is determined by the total force exerted by the filler. Grant D. Smith et al. [48] investigated the effect of filler-polymer interface on viscoelasticity by molecular dynamics simulations and found that the interaction at the interface of the two substances and the interface size greatly affect the viscoelasticity of the composites. Similarly, different shapes of fillers have different aspect ratios, which means that their effective volumes are different, and fillers with high effective volumes have certain advantages over low ones, which can reduce the permeation threshold of the fillers. When the filler volume fraction reaches a high value, the fillers are packed closely together and even form a filler network [49]. This drives the interaction between fillers to be greater than the interaction between the filler and the polymer [43]. And it is noteworthy that at low shear frequencies, the filler-filler interaction has a greater effect on the composite, while at high shear frequencies, the filler-polymer interaction has a greater effect on the composite [37]. The phenomenon of nonlinear variation of modulus of PNCs with strain amplitude after the addition of fillers is called Payne effect [40]. Several studies have demonstrated [41,50] that when the strain amplitude exceeds a certain value, the energy storage modulus decreases sharply while the loss modulus appears as a peak, a phenomenon that indicates the disruption of the formed filler network in the system, the disintegration of the filler clusters or other energy loss processes.

There is still a lack of theories to explain the viscoelasticity enhancement due to the addition of fillers, and this part is also less studied in simulation experiments, especially the different effects and mechanisms of modulus enhancement for different geometries of fillers. In this work, we investigated the viscoelasticity of PNCs respectively with spherical nanofillers (nanoparticles), rod nanofillers (nanorods) and sheet nanofillers (nanosheets) by molecular dynamics simulations, and investigated the effect of filler shape and filler size on the modulus enhancement of PNCs. Also, we discussed the modulus enhancement mechanism, which was compared with that proposed by Wei Hong et al. [51]. The study serves as a guide and explanation for relevant experiments, and provides ideas and insights for further fine quantification of theoretical work.

2. Models and methods

2.1. Models

In this project, a coarse-grained model [52] was chosen to build polymer nanocomposites filled with nanofillers. The system consists of polymer chains as well as different shapes of nanofillers. Each system has 1400 polymer chains and each polymer chain contains 30 beads. Each bead has a mass of $m = 1$ and a diameter of $\sigma = 1$. Compared to real polymer chains, the polymer chains in the coarse-grained model are already sufficient to display the static and dynamic characteristic behavior of long chains [53]. Our aim is not to study specific polymer chains, and the model setup falls within the range of parameters in the experiment that can capture typical polymer systems and all parameters are simplified by setting ε and σ equal to unit. A nanoparticle is a rigid ball consisting of 1 central bead and 6 vertex beads, with the vertex beads evenly spaced on the surface of the central bead; a nanorod is a rigid rod consisting of L beads; and a nanosheet is a rigid sheet consisting of $N \times N$ beads. When discussing the effects of filler shape and volume fraction (φ), we keep the individual filler masses of the three fillers as $m = 9$. A nanoparticle has a central bead of $m = 3$ and surface beads of $m = 1$ each. A nanorod is a rigid rod of 9 beads and a nanosheet is a rigid sheet of 3×3 beads, each set to $m = 1$. Snapshots of these three filler

models are shown in Fig. 1. When discussing the effect of filler size, the volume fraction of the filler was fixed at $\varphi = 10\%$. The nanoparticle is set to three sizes of $m = 4$, 9 and 16; for a mass of $m = 4$, the central bead is set as $m = 1$ and each surface bead is set as $m = 0.5$; for a mass of $m = 16$, the central bead is set as $m = 4$ and each surface bead is set as $m = 2$. The nanorod size is set as L = 4, 6 and 9, and each bead is $m = 1$. The nanosheet size is set as 3×3, 4×4 and 5×5, and each bead is $m = 1$. The model visualization can be seen in Fig. S6.

Dimensionless units are used in the simulation, where m is the unit of mass, σ the unit of length, and ε the unit of energy, and other physical quantities are derived from these three, such as time $\tau = \sigma\sqrt{m/\varepsilon}$, temperature $T = \varepsilon/k_b$, etc.

The inter-molecular and intra-molecular action potential functions are expressed using the Lennard-Jones (LJ) potential function with the following expressions:

$$E_{ij}(r) = \begin{cases} 4\varepsilon_{ij}\left[\left(\dfrac{\sigma}{r-\triangle}\right)^{12} - \left(\dfrac{\sigma}{r-\triangle}\right)^{6}\right] & r < r_{cutoff} + \varDelta \\ 0 & r \geq r_{cutoff} + \varDelta \end{cases} \quad (1)$$

where r_{cutoff} represents the distance $r - \triangle$ at which the interaction is truncated and shifted at the r_{cutoff} cutoff; and r is the distance between two interaction points. We set the polymer-polymer interaction to $\varepsilon_{pp} = 1.0$, the polymer-filler interaction to $\varepsilon_{pn} = 3.0$ and the filler-filler interaction to $\varepsilon_{nn} = 1.0$. The purpose of this setting is to construct a model for long-range attraction.

We use the FENE potential to describe the bonding interactions between the polymer chain beads:

$$E_{polymer-bond} = -0.5k_1R_0{}^2 \ln\left[1 - \left(\frac{r}{R_0}\right)^2\right] \quad (2)$$

where $k_1 = 30.0(\varepsilon/\sigma^2)$, $R_0 = 1.5\sigma$. Description of bonding interactions between filler beads in terms of rigid harmonic potential.:

$$E_{filler-bond} = k_2(r - r_0)^2 \quad (3)$$

where $k_2 = 10000(\varepsilon/\sigma^2)$, $r_0 = 1\sigma$.

The bond angle interactions between filler beads are expressed using the rigid harmonic potential:

$$E_{angle} = K[\cos(\theta) - \cos(\theta_0)]^2 \quad (4)$$

where $K = 10000\varepsilon$, the nanorod is set to $\theta_0 = 180°$, and the nanosheet is set to $\theta_0 = 90°$ and $\theta_0 = 180°$ to ensure that the filler can keep the same shape.

2.2. Methods

After obtaining the initial models of polymer chains and fillers, the simulated systems were equilibrated using NPT and NVT systems at $T^* = 1$ ($T_g \approx 0.5$) [54] and $P^* = 0.0$ in simulated time steps of $0.001\ \tau$. Periodic boundary conditions were used during the simulations. The dynamic equilibrium of different systems at high and low temperatures was carried out, and the equilibrium simulation time was $20000\ \tau$. The homogeneous simulation system with uniform dispersion and stable density was finally obtained, the volume of the simulate box was about $40*40*40\ \sigma^3$ and the number density was about 0.85. After determining the equilibrium of the system and the homogeneity of the filler dispersion by calculating the density and the radial distribution function (RDF), we used the non-equilibrium molecular dynamics (NEMD) method to simulate the dynamic oscillation of the material during processing. The shear velocity gradient in oscillatory shear is in the Y-direction, and the XZ-plane undergoes a periodic tilt deformation with a fixed shear frequency of $\upsilon = 0.01\ \tau^{-1}$. The shear stress during oscillatory shear can be expressed as
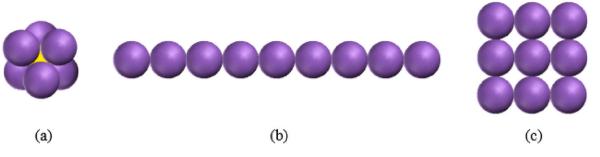
Fig. 1. Model visualization of (a) nanoparticles (b) nanorods and (c) nanosheets.

$$\sigma_{xy} = \gamma^0 [G' \sin(2\pi vt) + G'' \cos(2\pi vt)] \tag{5}$$

where G' denotes the energy storage modulus of the system and G'' denotes the loss modulus of the system. All of our simulation experiments are performed using LAMMPS, a large-scale atomic-molecular integrated parallel simulation software.

3. Results and discussion

3.1. Influence of filler shape and filler size on the viscoelasticity of PNCs

Firstly, we investigated the effect of filler shapes of nanoparticles, nanorods and nanosheets on the viscoelasticity of PNCs systems.

It has been shown that the dispersion effect of fillers can seriously affect the material properties of PNCs [11,55,56]. We demonstrated the uniform dispersion of the filler in the composite by characterizing the radial distribution function (RDF) of the filler, as shown in Fig. S1. Fig. S2 demonstrates the energy storage modulus and loss modulus versus shear strain amplitude for PNCs with different shapes of fillers, and all PNCs have a distinct low-strain energy storage modulus plateau, that is, a linear viscoelastic region. With the increase of filler amount, the plateau region becomes narrower and the energy storage modulus increases. Comparing the effects of the shape of three fillers on the viscoelasticity of PNCs at the same volume fraction, Fig. 2(a), it can be seen that nanorods have the best effect on the modulus enhancement of PNCs, which is slightly better than nanosheets, and nanoparticles play the weakest role in the modulus enhancement. According to the reports [47], it is known that both nanorods and nanosheets have strong adsorption force on polymer chains. In this work, it is ensured that the aspect ratio of nanorods is larger than that of nanosheets when the mass of individual filler is the same; therefore, at the same volume fraction, the adsorption force of nanorods is greater than that of nanosheets and then the nanorod is more restrictive to polymer chain movement [57], which largely enhances the modulus of PNCs. When the filler reaches the permeation threshold [58,59] then the effect of further increase in filler

on modulus enhancement is diminished. As shown in Fig. 2(b), the loss modulus of PNCs respectively filled with the three shapes of fillers follows the same trend as the energy storage modulus. From Fig. S2, it can be seen that the nanorod has the lowest permeation threshold and is the easiest to form a filler network, followed by the nanosheet, and the nanoparticle is less likely to form a filler network. At low strain, the energy losses of PNCs respectively filled with nanorods and nanosheets at high filler amount are even lower than those at low filler amount, which can be attributed to the fact that filler networks formed by increased filler greatly shackles the polymer chains and makes the system form a solid-like phase, which enhances the modulus and also relatively reduces the slip loss of polymer chains on the filler surface.

The effect of filler size (model visualization is shown in Fig. S6) on the viscoelasticity of PNCs is shown in Fig. 3. The energy storage modulus of PNCs filled with nanoparticles decreases with increasing filler size, which can be attributed to the decrease in the number of fillers at the same volume fraction. The reduction in the total effective specific surface area of the filler reduces its interaction area with the polymer, while the nanoparticle itself has a weaker ability to confine the polymer chains, which reduces the strength of the filler-polymer network formed by the adsorption of polymer chains by the filler and ultimately leads to a decrease in modulus. The energy storage modulus is almost constant with the filler size for PNCs respectively filled with nanorods and nanosheets. However, the increase of the filler size makes the number of fillers smaller, and in this case the energy storage modulus of the PNCs system can still be maintained about the same, which means that the increase of the filler size of nanorods and nanosheets has the same effect on the strength of the adsorption of polymer chains in the PNCs system to form the filler-polymer network as the increase of the filler volume fraction. In other words, when the filler volume fraction is the same, increasing the filler size can enhance the modulus of PNCs to some extent. Comparing the three fillers, the nanorod always has the strongest effect on the modulus enhancement, which is due to the fact that the nanorod has the largest aspect ratio and the largest effective area of interaction with the polymer chains in the model construction in this
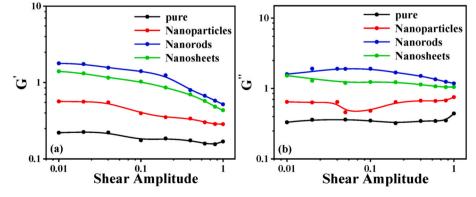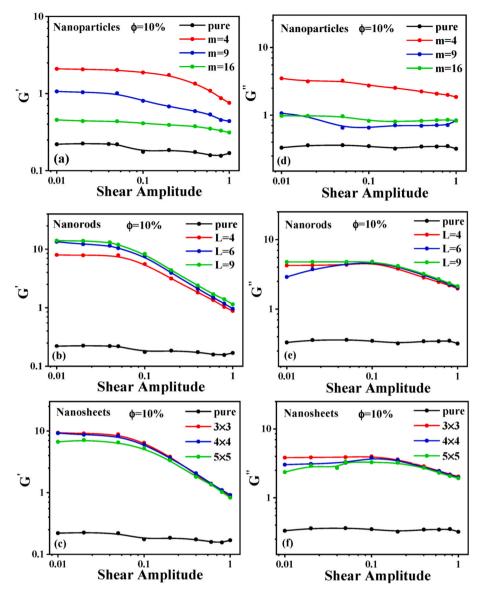

Fig. 2. Plots of (a) energy storage modulus and (b) loss modulus as a function of shear amplitude for PNCs respectively filled with nanoparticles, nanorods and nanosheets, at φ = 5%, $v = 0.01\ \tau^{-1}$.

Fig. 3. Variation of energy storage modulus with shear amplitude for PNCs respectively filled with different sizes of (a) nanoparticles, (b) nanorods and (c) nanosheets; variation of loss modulus with shear amplitude for PNCs respectively filled with different sizes of (d) nanoparticles, (e) nanorods and (f) nanosheets. $v = 0.01\ \tau^{-1}$.

work. The loss modulus has a similar trend to the storage modulus.

In order to compare the Payne effect appearing in each system, we quantified the Payne effect [60].

$$G^* = \left(G'_{5\%} - G'_{100\%}\right) / G'_{5\%} \qquad (6)$$

where $G'_{5\%}$ and $G'_{100\%}$ denote the energy storage modulus at shear am-
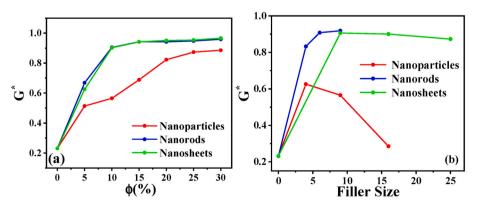

Fig. 4. Quantified Payne effect of PNCs filled with different shapes of fillers as a function of (a) volume fraction and (b) the size of the filler.

plitudes of 5% and 100%, respectively; G* denotes the quantified Payne effect. According to Equation (6), we obtain the quantified Payne effect as a function of filler volume fraction and filler size as shown in Fig. 4. It can be seen from the Fig. 4(a) that the Payne effects of PNCs respectively filled with nanorods and nanosheets are both most sensitive to the filler amount (PNCs filled with nanorods is slightly more sensitive than PNCs filled with nanosheets), and the Payne effect is already significant at smaller filler amounts. In contrast, the Payne effect for PNCs filled with nanoparticles requires a higher filler amount before a significant Payne effect occurs. Also from Fig. 4(b), it can be seen that the Payne effect of PNCs filled with nanoparticles decreases with increasing filler size. The Payne effects of PNCs respectively filled with nanorods and nanosheets do not vary much with filler size and are only affected by size to a small extent. The trend of the quantified Payne effect G* is consistent with the change in modulus.

3.2. Modulus enhancement mechanism

The first step was to calculate the relaxation times of polymer chains in pure polymers and PNCs, using the method of Rouse dynamics analysis. Here the simple positive mode analysis of polymer chains was first performed [61],

$$X_p(t) = \sqrt{\frac{2}{L}} \sum_{i=1}^{L} \cos\left(p\pi \frac{i-1/2}{L}\right) r_i(t) \qquad (7)$$

In Equation (7), $X_p(t)$ is the pth simple positive mode function of the polymer chain. The p is the mode number, and its maximum value cannot exceed the number of chain lengths. The L denotes the polymer chain length, which is the total number of beads in a polymer chain; in this work, L = 30. The $r_i(t)$ denotes the coordinates of the polymer beads in the three-dimensional space. By the simple positive mode analysis, we further calculate to give the autocorrelation function $A_p(t)$ of the simple positive mode function that,

$$A_p(t) = \frac{\langle X_p(t) \cdot X_p(0) \rangle}{\langle X_p(0) \cdot X_p(0) \rangle} \qquad (8)$$

where the pointed brackets <> denote the average value of the coefficient of integration for all polymer chains and fillers. We can obtain the relaxation time by fitting the autocorrelation function $A_p(t)$ as a decay exponential function. We use the modified equation proposed by previous researchers [48,62] to fit the autocorrelation function $A_p(t)$ for PNCs in different modes:

$$A_p(t) = C \cdot \exp\left[-\left(\frac{t}{\tau_p}\right)^\beta\right] + (1-C) \cdot \exp\left[-\frac{t}{\tau_1}\right] \qquad (9)$$

where τ_p is the relaxation time of the sought pth mode, β is the fitting parameter; C and τ_1 are additional fitting parameters indicating the decay of two classes of exponential functions.

Fig. 5 gives a plot of the $A_p(t)$ function calculated for different systems with 5% volume fraction, which can be seen that the three fillers can affect the relaxation of polymer chains to different extent. It is worth noting that the relaxation time of PNCs with higher filler amount is too long, so the relaxation process cannot be fully observed. And Fig. S7 shows the time dependent function of the whole chain relaxation in PNCs filled with different size fillers, which is, the autocorrelation function $A_p(t)$ at p = 1. It can be seen that the degree of whole-chain motion restriction of polymer chains in different PNCs systems decreases and then increases with increasing filler size. This can be attributed to the fact that at the same filler volume fraction, the increase in filler size decreases the number of fillers and reduces the strength of the limiting effect on polymer chain motion, which is similar to the effect of decreasing the volume fraction of fillers. However, with the further increase in filler size, the limiting effect of filler geometrical constraints on polymer chains is much greater than the limiting effect of increasing the volume fraction of fillers. Therefore, despite the decrease in the number of fillers due to the increase in size, the restriction of polymer chain motion can still be increased.
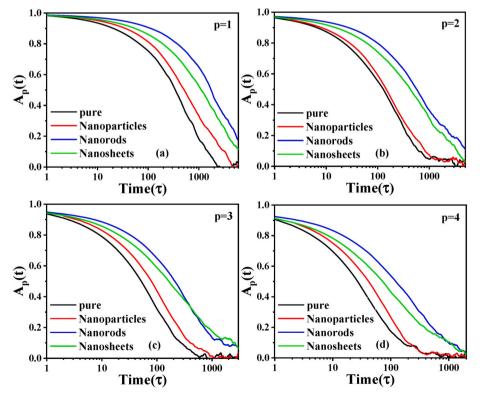

Fig. 5. Plots of $A_p(t)$ functions for the four modes (a) p = 1 (b) p = 2 (c) p = 3 (d) p = 4 of the PNCs filled with different shape fillers at φ = 5%.

We compared the values of relaxation time and energy storage modulus for pure polymer and PNCs filled with 5% volume fraction of filler, as shown in Fig. 6(a). The results show that the relaxation times of PNCs respectively filled with nanoparticles, nanorods and nanosheets at $\varphi = 5\%$ are 2.6, 7.4 and 5.6 times higher than those of the pure polymer system, respectively; and their moduli in the plateau region are 2.56, 7.18 and 5.48 times higher than those of the pure polymer system, respectively. These data are consistent with the results predicted by Rouse dynamics theory. Subsequently, we also performed the fitting of exponential relationship between relaxation time and mode number p. According to the Rouse dynamics theory, the relaxation time and the mode number show an exponential relationship with a power of −2, that is, $\tau_p \sim p^{-2}$. As shown in Fig. 6(b), the fitted exponents for the pure polymer system are all around −2. Meanwhile, when $\varphi = 10\%$, the deviation of the fitted exponents from −2 becomes large for PNCs respectively filled with nanorods and nanosheets, indicating that the Rouse motion of polymer chains in the system contributes less to the enhancement of the modulus; while the fitted exponents of PNCs filled with nanoparticles are closest to −2.

Further, we list the fitted exponents in Tables 1 and 2, respectively. From Table 1, we can clearly see that all the fitted exponents of PNCs respectively filled with three shapes of fillers at low filler amount fit the analytical category of the Rouse model. PNCs filled with nanorods deviating the most from −2, indicates that nanorods have the greatest restriction on the Rouse motion of the polymer chains, followed by nanosheets. The relaxation of the polymer chains in the PNCs respectively filled with nanorods and nanosheets no longer fits the scope of the Rouse dynamics model analysis with the increase of the filler amount (the circled parts in Table 1). The above analysis shows that the polymer chains in PNCs respectively filled with nanorods and nanosheets usually follow Rouse dynamics at lower filler amount, while the polymer chains in PNCs filled with nanoparticles are always more consistent with the Rouse dynamics model. It is clear from Table 2 that the results of the Rouse analysis are consistent with the enhancement of the dynamic modulus, except for the PNCs filled with nanoparticles; the larger the size the longer its relaxation time and the farther it deviates from the fitted exponent −2 in the Rouse theoretical model. The polymer chains within the PNCs filled with nanoparticles always fit the Rouse dynamics analysis category, and the fitted exponents hardly deviate with filler size, indicating that the nanoparticle hardly hinders the relaxation and the Rouse motion of the polymer chains in the system.

The significant increase in relaxation time due to increased filler amount can be attributed to the increased binding of the filler to the polymer chains, and we calculated the mean square radius of gyration $\langle R_g^2 \rangle$ and mean square end distance $\langle R_{ee}^2 \rangle$ of the polymer chains. As shown in Fig. 7, the stretching of the polymer chains shows that the nanorod has the strongest constraint on the polymer chains at moderate amount, while the nanosheet has the strongest constraint when the permeation threshold is exceeded. PNCs respectively filled with nanorods and

Table 1
Values of exponential -k between relaxation time τ_p and mode number p for PNCs respectively filled with different shape fillers ($\tau_p \sim p^{-k}$).

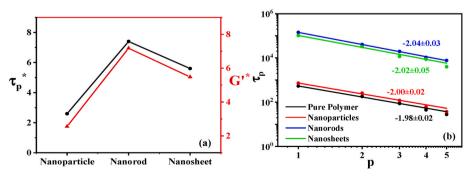| φ (%)	Nanoparticles	Nanorods	Nanosheets
0	1.99 ± 0.02	1.99 ± 0.02	1.99 ± 0.02
5	2.00 ± 0.02	2.02 ± 0.03	2.01 ± 0.02
10	2.00 ± 0.02	2.04 ± 0.03	2.02 ± 0.05
15	2.01 ± 0.01	2.18 ± 0.04	2.16 ± 0.03
20	2.03 ± 0.03	2.27 ± 0.07	2.23 ± 0.06

Table 2
Values of exponential -k between relaxation time τ_p and mode number p for PNCs respectively filled with different size fillers ($\tau_p \sim p^{-k}$).
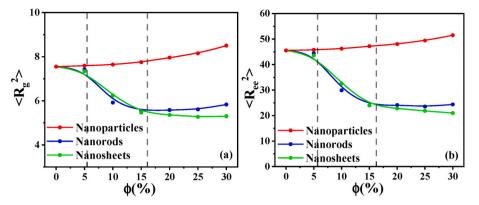
Nanofiller Size	Nanoparticles	Nanorods	Nanosheets
0	1.99 ± 0.02	1.99 ± 0.02	1.99 ± 0.02
4	2.00 + 0.01	2.01 + 0.02	2.01 + 0.03
6	–	2.02 ± 0.02	–
9	2.00 ± 0.02	2.04 ± 0.03	2.02 ± 0.05
16	2.00 + 0.01	2.08 + 0.02	2.06 + 0.04
25	–	–	2.08 ± 0.05

nanosheets are consistent with the Rouse dynamics analysis, where the modulus enhancement originates from the polymer chain Rouse dynamics at lower filler amount, the constraint of the polymer chains by the filler at moderate filler amount; and at high filler amount the enhancement of modulus is attributed to filler network [63]. For this theory, PNCs respectively filled with nanorods and nanosheets fit it very well, but PNCs filled with nanoparticles cannot be explained using this theory. It can be seen from the Fig. 7 that the polymer chains in PNCs filled with nanoparticles become more stretched with the increase of filler volume fraction. We calculated the average number of polymer chains associated with each nanofiller and the average number of nanofillers associated with each polymer chain, as shown in Fig. S11. It can be seen that as the volume fraction increases, the number of polymer chains adsorbed by each nanoparticle decreases while each polymer chain is adsorbed by more nanoparticles. It indicates that in the system of PNCs filled with nanoparticles, the polymer chains are absorbed and stretched by more fillers due to the uniform dispersion of the fillers. The opposite is true in the PNCs systems respectively filled with nanorods and nanosheets. We also give the mean square displacement (MSD) plots for the different systems at 5% and 15% volume fraction in Fig. S12 in the supporting information file.
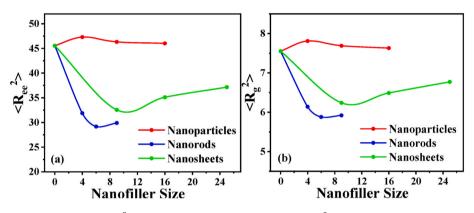
As shown in Fig. 8, it is found that the effect of filler size on the polymer chains is consistent with the enhancement of dynamic modulus within a certain range, that is, the larger the size the more restrictive the polymer chains are. Both the mean square end distances and the mean square radius of gyration of polymer chains in PNCs filled with nanoparticles became smaller with increasing filler size due to the decrease in the number of fillers and the weaker geometrical constraint imposed on

Fig. 6. (a) Ratio of relaxation time τ_p and energy storage modulus G′ of PNCs filled with different shape fillers to that of pure polymer at $\varphi = 5\%$, where $\tau_p^* = \tau_p(i)/\tau_p(polymer)$, $G'^* = G'(i)/G'(polymer)$, i means nanoparticles, nanorods, nanosheets. (b) Fitting relaxation time of PNCs filled with different shape fillers at $\varphi = 10\%$.

Fig. 7. Variation of (a) mean square radius of gyration $\langle R_g^2 \rangle$ and (b) mean square end distance $\langle R_{ee}^2 \rangle$ with filler volume fraction for PNCs respectively filled with different shape fillers.

Fig. 8. Variation of (a) mean square end distance $\langle R_{ee}^2 \rangle$ and (b) mean square radius of gyration $\langle R_g^2 \rangle$ with filler size for PNCs respectively filled with different shape fillers.

the polymer chains by nanoparticles. The mean square end distances and mean square radii of gyration of polymer chains in PNCs respectively filled with nanorods and nanosheets first become smaller and then larger with the increase of filler size. The two distances first become smaller because the geometrical constraint of the polymer chains is enhanced by the increase in size of the nanorod and the nanosheet, and then become larger because the number of fillers is reduced too much and the fillers are dispersed further apart, weakening the restraint of the polymer chains. Therefore, the effect of filler size on the modulus of PNCs is to narrow the Rouse dynamics region and the system will enter the chain bound region at a smaller volume fraction.

The above theory is proposed based on the analysis of equilibrium polymer dynamics, and we further analyze the interaction energy fluctuates under oscillatory shear. The difference between the highest and lowest interaction energy in one cycle is taken to characterize the energy loss of the system during dynamic oscillatory shear, as shown in Fig. 9. We calculated the interaction energy differences of polymer-filler, polymer-polymer and filler-filler during oscillatory shear. The polymer-polymer interaction energy differences (Fig. S3) of the three PNCs did not vary significantly with the volume fraction of the filler, indicating that the increase of the filler had little effect on the friction loss between the polymers. In addition, the polymer-filler interaction energy difference (Fig. S4) and the filler-filler interaction energy difference (Fig. S5) become larger with increasing shear amplitude, indicating that increasing shear amplitude makes the friction between the filler and the polymer increase, so the system's energy loss increases and the modulus decreases [13,36,43,64]. The interaction energy difference diagram confirms that the friction loss between the particles in the system leads to the Payne effect and that the polymer-filler friction loss is the dominant one. From Fig. 4(a), it is known that the Payne effect is
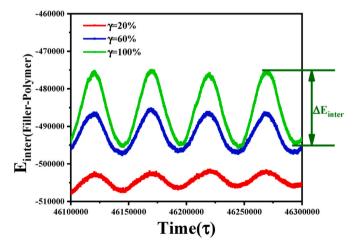

Fig. 9. Schematic diagram of the filler-polymer interaction energy of the system during oscillatory shear.

evident for all three types of fillers at $\varphi = 20\%$. Comparing the interaction energy difference of PNCs respectively filled with the three shape fillers at this time, it can be seen that the friction losses of PNCs respectively filled with nanorods and nanosheets mainly come from the polymer-filler interactions because of the formation of filler network; while the nanoparticle is difficult to form a filler network to shackle the polymer chains, which makes the friction loss between polymer chains become more, as shown in Fig. 10.

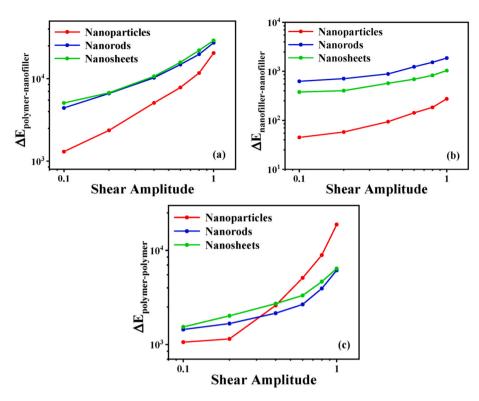After exploring the influence and mechanism of the shape and size of

Fig. 10. Variation of (a) polymer-filler (b) filler-filler (c) polymer-polymer interaction energy difference with shear amplitude for PNCs respectively filled with three shape fillers during oscillatory shear, $\varphi = 20\%$.

three types of fillers, namely nanoparticles, nanorods and nanosheets, on the viscoelasticity of PNCs, it can be found that for PNCs respectively filled with nanorods and nanosheets: at low amount, the contribution of the modulus of PNCs is mainly due to the relaxation of polymer chains in the Rouse dynamics mode; when moderate amount are reached, the main contribution of the modulus enhancement comes from the adsorption of the filler to the polymer chains, which limits the polymer chain movement; the system no longer has a large increase in modulus when the filler amount increases to a certain amount because fillers are in contact with each other and form a filler network that can directly transfer stress. This is in agreement with the work of Wei Hong et al. [63]. In contrast, the Rouse dynamics region as well as the chain confinement region of both PNCs filled with nanorods and PNCs filled with nanosheets become narrower as the filler size increases. For PNCs filled with nanoparticles, the modulus enhancement is always the Rouse dynamics of polymer chains as the main source.

3.3. Viscoelasticity of PNCs filled with nanoparticles of different interfacial degrees

In the above results, the viscoelastic variation of the PNCs filled with nanoparticles is consistently inconsistent with the PNCs respectively filled with nanorods and the nanosheets. We redesigned two types of cluster-type nanoparticles with different degrees of interface. One is a cluster spherical type with the number of surface beads increased to 12, called Multi-interface Nanoparticles (MNPs); the other is directly set as a single large sphere without surface beads, called Uni-interface Nanoparticles (UNPs). The nanoparticle we originally used is called Olig-interface Nanoparticles (ONPs). The model is visualized in Fig. S6, the center bead mass of MNPs is set to m = 3 and the surface bead mass is set to m = 0.5 to ensure a total mass of 9; ONPs are set to a large bead with a mass of 9.

The energy storage modulus and loss modulus were calculated for the PNCs respectively filled with three types of nanoparticles (Fig. S8). As shown in Fig. 11, the improvement of modulus by MNPs is much
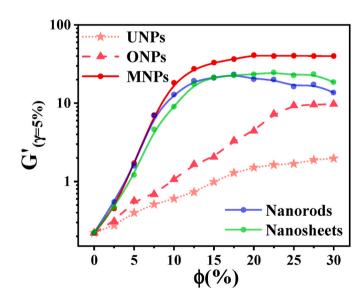

Fig. 11. Variation of energy storage modulus with volume fraction at $\gamma = 5\%$ for PNCs respectively filled with different interfacial degrees nanoparticles.

higher than that by ONPs. When the filler amount is increased until the modulus does not change much, the modulus of energy storage of PNCs filled with MNPs in the platform region can reach about twice of that of PNCs respectively filled with nanorods and nanosheets with the same volume fraction at this time. At the same time, it can be found that the improvement of modulus by UNPs is inferior to that of the original ONPs, and the dynamic modulus does not even increase to a relatively stable value with the increase of filler amount. It can also be seen that at high volume fractions, the enhancement of nanosheets is better than that of nanorods. Meanwhile, the energy storage modulus of PNCs filled with nanorods slightly decreases, which can be attributed to the fact that

the increase in the degree of connection between the fillers when the volume fraction of nanorods increases (this can be observed from the RDF diagram of nanorods in Fig. S1, where the peak at 1 σ at higher volume fractions of filler exceeds 1, indicating that each nanorod is in contact with another nanorod), resulting in a decrease in the effective interaction area of nanorods, thus the stress transfer efficiency between the filler and the polymer matrix decreases; the contribution of the polymer matrix in the modulus decreases and the filler-filler interaction in the system setup is lower than the filler-polymer interaction, so the modulus enhancement is gradually weakened.

As shown in Fig. S9, the autocorrelation function $A_p(t)$ calculated in the Rouse model analysis shows that the whole chain motion of polymers in PNCs filled with MPNs at mode number p = 1 becomes significantly slower and its relaxation time increases greatly. When the degree of interface increases, the interfacial interaction between nanoparticles and polymer chains becomes stronger, making nanoparticles more capable of adsorbing polymer chains, and therefore the relaxation time of polymer chains increases substantially. The effect of MNPs is consistent with the effect of nanorods and nanosheets, both of which gradually deviate from the Rouse dynamics mode analysis after the amount is increased for the system. What can also be seen in Table 3 is that the amount of UNPs increases up to 20% and the PNCs still conform to the Rouse dynamics mode analysis.

The motion of the polymer chains is a good indication of the constraining effect of the filler on the polymer, so we calculated the mean square displacement (MSD) of the polymer. It can be seen from Fig. 12 that the MSD of the MNPs system is lower than that of the other two systems, indicating that the enhanced interfacial interaction limits the polymer chain motion well, but the chain structure is still stretched (Fig. S10). From the above analysis, it can be seen that with the increase of the filler volume fraction, the main source of the modulus enhancement of the PNCs filled with MNPs gradually changes from the Rouse dynamics motion of the polymer chains to the constraining effect of the filler on the polymer chains.

4. Conclusions

In this work, we investigated the viscoelasticity of PNCs respectively filled with nanoparticles, nanorods and nanosheets and compared the effects of filler shape and filler size. The nanorod has the most outstanding ability to increase the modulus of PNCs among the three, followed by the nanosheet. These two shapes of fillers have high specific surface area and can restrict polymer chain movement well, thus increasing the modulus. Nanorods and nanosheets have a lower permeation threshold than nanoparticles and can form the packing network faster. The increase of filler size can increase the modulus of the system and has little effect on Payne effect.

Through the analysis of Rouse dynamics, polymer chain dynamics and energy loss during shear for different systems, the investigation revealed that the modulus enhancement mechanism of PNCs respectively filled with nanorods and nanosheets can be divided into three parts: Rouse dynamics at low filler amount, chain confinement of the filler at medium filler amount, and filler network at high filler amount [63]. And increasing the filler size also increases the modulus of the system to some extent, but makes the Rouse dynamics region and chain confinement region narrower and the permeation threshold lower. The nanoparticle can have a good modulus enhancement rapidly with increasing filler amount only when its interfacial effect is strong. In contrast, Rouse dynamics of polymer chains has been the main source of modulus enhancement of PNCs filled with nanoparticles of low interfacial interactions.

CRediT authorship contribution statement

Dandan Luo: Data curation, Formal analysis, Investigation, Methodology. **Haoyu Wu:** Data curation, Formal analysis. **Haoxiang Li:**

Table 3

Values of exponential -k between relaxation time τ_p and mode number p for PNCs respectively filled with three types of nanoparticles ($\tau_p \sim p^{-k}$).

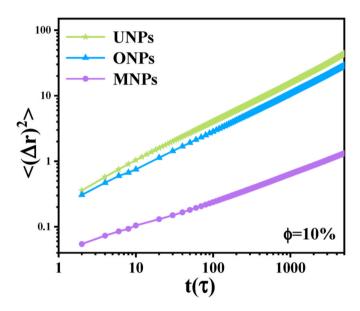| φ (%)	UNPs	ONPs	MNPs
0	1.99 ± 0.02	1.99 ± 0.02	1.99 ± 0.02
5	1.99 ± 0.02	2.00 ± 0.02	2.02 ± 0.01
10	2.00 ± 0.02	2.00 ± 0.02	2.07 ± 0.05
15	2.00 ± 0.01	2.01 ± 0.01	2.29 ± 0.09
20	2.01 ± 0.01	2.03 ± 0.02	2.42 ± 0.11

Fig. 12. MSD of PNCs respectively filled with different interfacial degrees nanoparticles.

Investigation, Methodology. **Wenfeng Zhang:** Formal analysis, Methodology. **Liqun Zhang:** Project administration, Funding acquisition, Supervision, Writing – original draft, Writing – review & editing. **Yangyang Gao:** Investigation, Methodology, Project administration, Funding acquisition, Supervision, Writing – original draft, Writing – review & editing.

Declaration of competing interest

The authors declare that they have no known competing financial interests or personal relationships that could have appeared to influence the work reported in this paper.

Acknowledgements

Appendix A. Supplementary data

Supplementary data to this article can be found online at https://doi.org/10.1016/j.polymer.2022.124750.

References

[1] J. Aghazadeh Mohandesi, A. Refahi, E. Sadeghi Meresht, S. Berenji, Effect of temperature and particle weight fraction on mechanical and micromechanical properties of sand-polyethylene terephthalate composites: a laboratory and discrete element method study, Compos. B Eng. 42 (6) (2011) 1461–1467.

[2] Ji-Zhao Liang, Reinforcement and quantitative description of inorganic particulate-filled polymer composites, Compos. B Eng. 51 (Complete) (2013) 224–232.

[3] M. Bhattacharya, A.K. Bhowmick, Synergy in carbon black-filled natural rubber nanocomposites. Part I: mechanical, dynamic mechanical properties, and morphology, J. Mater. Sci. 45 (22) (2010) 6126–6138.

[4] R. Sengupta, S. Chakraborty, S. Bandyopadhyay, S. Dasgupta, A.S. Deuri, A short review on rubber/clay nanocomposites with emphasis on mechanical properties, Polym. Eng. Sci. 47 (11) (2007) 1956–1974.

[5] D. Bikiaris, Can nanoparticles really enhance thermal stability of polymers? Part II: an overview on thermal decomposition of polycondensation polymers, Thermochim. Acta 523 (1) (2011) 25–45.

[6] A. Boudenne, L. Ibos, M. Fois, J.C. Majesté, E. Géhin, Electrical and Thermal Behavior of Polypropylene Filled with Copper Particles, Composites Part A: Applied Science and Manufacturing, 2005.

[7] S. Takahashi, Y. Imai, A. Kan, Y. Hotta, H. Ogawa, Dielectric and thermal properties of isotactic polypropylene/hexagonal boron nitride composites for high-frequency applications, J. Alloys Compd. (2014).

[8] X. Xiong, J. Wang, H. Jia, E. Fang, L. Ding, Structure, thermal conductivity, and thermal stability of bromobutyl rubber nanocomposites with ionic liquid modified graphene oxide, Polym. Degrad. Stabil. 98 (11) (2013) 2208–2214.

[9] A.T. Mou'ad, A.M. Ali, S.H. Ahmad, L. Yu, Influence of multiwalled carbon nanotubes content on thermal conductivity of polyactic acid/liquid natural rubber nanocomposite, World J. Eng. (2016).

[10] B. Olalla, C. Carrot, R. Fulchiron, I. Boudimbou, E. Peuvrel-Disdier, Analysis of the influence of polymer viscosity on the dispersion of magnesium hydroxide in a polyolefin matrix, Rheol. Acta 51 (3) (2012) 235–247.

[11] S.L. Mills, G.C. Lees, C.M. Liauw, S. Lynch, Dispersion assessment of flame retardant filler/polymer systems using a combination of X-ray mapping and multifractal analysis, Polym. Test. 21 (8) (2002) 941–947.

[12] A. Subik, A. Smejda-Krzewicka, K. Strzelec, Curing behaviors, mechanical and dynamic properties of composites containing chloroprene and butadiene rubbers crosslinked with nano-iron(III) oxide, Polymers 13 (6) (2021) 853.

[13] F. Peinado, E. Medel, R. Silvestre, A. Garcia, Open-grade wearing course of asphalt mixture containing ferrite for use as ferromagnetic pavement, Compos. B Eng. 57 (2014) 262–268.

[14] F. Qin, C. Brosseau, A review and analysis of microwave absorption in polymer composites filled with carbonaceous particles, J. Appl. Phys. 111 (6) (2012) 4–227.

[15] A. Hunyek, C. Sirisathitkul, Electromagnetic and dynamic mechanical properties of extruded cobalt ferrite-polypropylene composites, Polym. Plast. Technol. Eng. 50 (6) (2011) 593–598.

[16] F. Danes, B. Garnier, T. Dupuis, Predicting, measuring, and tailoring the transverse thermal conductivity of composites from polymer matrix and metal filler, Int. J. Thermophys. 24 (3) (2003) 771–784.

[17] T. Tanaka, M. Kozako, K. Okamoto, Toward high thermal conductivity nano micro epoxy composites with sufficient endurance voltage, J. Int. Counc. Electr. Eng. 2 (1) (2012) 90–98.

[18] P.S. Thomas, A.A. Abdullateef, M.A. Al-Harthi, M.A. Atieh, S. De, M. Rahaman, T. Chaki, D. Khastgir, S. Bandyopadhyay, Electrical properties of natural rubber nanocomposites: effect of 1-octadecanol functionalization of carbon nanotubes, J. Mater. Sci. 47 (7) (2012) 3344–3349.

[19] O. Saravari, A. Boonmahitthisud, W. Satitnaithum, S. Chuayjuljit, Mechanical and electrical properties of natural rubber/carbon nanotube nanocomposites prepared by latex compounding, Adv. Mater. Res. 664 (2013) 543–546.

[20] R. Moucka, J. Vil Ca Kova, N.E. Kazantseva, A.V. Lopatin, P. Sana, The influence of interfaces on the dielectric properties of MnZn-based hybrid polymer composites, J. Appl. Phys. 104 (10) (2008) 2224.

[21] S.-Y. Fu, X.-Q. Feng, B. Lauke, Y.-W. Mai, Effects of particle size, particle/matrix interface adhesion and particle loading on mechanical properties of particulate–polymer composites, Compos. B Eng. 39 (6) (2008) 933–961.

[22] S.K. Bhattacharya, R.T. Rao, Next generation integral passives: materials, processes, and integration of resistors and capacitors on PWB substrates, J. Mater. Sci. Mater. Electron. 11 (3) (2000) 253–268.

[23] A. Kutvonen, G. Rossi, S.R. Puisto, N. Rostedt, T. Ala-Nissila, Influence of nanoparticle size, loading, and shape on the mechanical properties of polymer nanocomposites, J. Chem. Phys. 137 (21) (2012) 214901.

[24] T. Honek, B. Hausnerova, P. Saha, Relative viscosity models and their application to capillary flow data of highly filled hard-metal carbide powder compounds, Polym. Compos. 26 (1) (2010) 29–36.

[25] B. Hausnerova, N. Honkova, T. Kitano, P. Saha, Superposed flow properties of ceramic powder-filled polymer melts, Polym. Compos. 30 (8) (2009) 1027–1034.

[26] S. Zürcher, T. Graule, Influence of dispersant structure on the rheological properties of highly-concentrated zirconia dispersions, J. Eur. Ceram. Soc. 25 (6) (2005) 863–873.

[27] D.M. Kalyon, S. Aktaş, Factors affecting the rheology and processability of highly filled suspensions, Ann. Rev. Chem. Biomol. Eng. 5 (2014) 229–254.

[28] S.K. Bhattacharya, R.R. Tummala, Next generation integral passives: materials, processes, and integration of resistors and capacitors on PWB substrates, J. Mater. Sci. Mater. Electron. 11 (3) (2000) 253–268.

[29] B. Wang, Q. Wang, L. Li, Morphology and properties of highly talc-and CaCO3-filled poly (vinyl alcohol) composites prepared by melt processing, J. Appl. Polym. Sci. 130 (5) (2013) 3050–3057.

[30] M. Tarfaoui, S. Choukri, A. Neme, Effect of fibre orientation on mechanical properties of the laminated polymer composites subjected to out-of-plane high strain rate compressive loadings, Compos. Sci. Technol. 68 (2) (2008) 477–485.

[31] G.D. Smith, D.B. rov, L. Li, O. Byutner, A molecular dynamics simulation study of the viscoelastic properties of polymer nanocomposites, J. Chem. Phys. 117 (20) (2002) 9478–9489.

[32] X. Chen, J. Gug, M.J. Sobkowicz, Role of polymer/filler interactions in the linear viscoelasticity of poly(butylene succinate)/fumed silica nanocomposite, Compos. Sci. Technol. 95 (2014) 8–15.

[33] N. Ning, S. Fu, W. Zhang, F. Chen, K. Wang, H. Deng, Q. Zhang, Q. Fu, Realizing the enhancement of interfacial interaction in semicrystalline polymer/filler composites via interfacial crystallization, Prog. Polym. Sci. 37 (10) (2012) 1425–1455.

[34] X. Zhai, Y. Chen, D. Han, J. Zheng, L. Zhang, New designed coupling agents for silica used in green tires with low VOCs and low rolling resistance, Appl. Surf. Sci. 558 (5) (2021) 149819.

[35] Y. Li, B. Han, S. Wen, Y. Lu, H. Yang, L. Zhang, L. Liu, Effect of the Temperature on Surface Modification of Silica and Properties of Modified Silica Filled Rubber Composites, Composites Part A: Applied Science and Manufacturing, 2014.

[36] B. Hausnerova, N. Honkova, T. Kitano, P. Saha, Superposed flow properties of ceramic powder-filled polymer melts, Polym. Compos. 30 (8) (2009) 1027–1034.

[37] M.M. Rueda, M.-C. Auscher, R. Fulchiron, T. Perie, G. Martin, P. Sonntag, P. Cassagnau, Rheology and applications of highly filled polymers: a review of current understanding, Prog. Polym. Sci. 66 (2017) 22–53.

[38] H.A. Barnes, A review of the rheology of filled viscoelastic systems, Rheol. Rev. (2003) 1–36.

[39] C. Lang, M.P. Lettinga, Shear flow behavior of bidisperse rodlike colloids, Macromolecules 53 (7) (2020) 2662–2668.

[40] P. Cassagnau, Melt rheology of organoclay and fumed silica nanocomposites, Polymer 49 (9) (2008) 2183–2196.

[41] C. Carrot, J.-C. Majesté, B. Olalla, R. Fulchiron, On the use of the model proposed by Leonov for the explanation of a secondary plateau of the loss modulus in heterogeneous polymer–filler systems with agglomerates, Rheol. Acta 49 (5) (2010) 513–527.

[42] D.W. Chae, B.C. Kim, Thermal and rheological properties of highly concentrated PET composites with ferrite nanoparticles, Compos. Sci. Technol. 67 (7) (2007) 1348–1352.

[43] T. Kaully, A. Siegmann, D. Shacham, Rheology of highly filled natural CaCO3 composites. II. Effects of solid loading and particle size distribution on rotational rheometry, Polym. Compos. 28 (4) (2007) 524–533.

[44] Y. Li, M. Kröger, W.K.J.M. Liu, Nanoparticle Geometrical Effect on Structure, Dynamics and Anisotropic Viscosity of Polyethylene Nanocomposites, vol. 45, 2012, pp. 2099–2112, 4.

[45] D. Zhao, S. Ge, E. Senses, P. Akcora, J. Jestin, S.K.J.M. Kumar, Role of Filler Shape and Connectivity on the Viscoelastic Behavior in Polymer Nanocomposites, vol. 48, 2015, pp. 5433–5438, 15.

[46] W. Cui, W. You, W.J.M. Yu, Mechanism of mechanical reinforcement for weakly attractive nanocomposites in, Glassy Rubbery States 54 (2) (2021) 824–834.

[47] Y. Gao, J. Liu, J. Shen, Y. Wu, L. Zhang, Influence of Various Nanoparticle Shapes on the Interfacial Chain Mobility: A Molecular Dynamics Simulation 16, 2014, pp. 21372–21382, 39.

[48] G.D. Smith, D. Bedrov, L. Li, O. Byutner, A molecular dynamics simulation study of the viscoelastic properties of polymer nanocomposites, J. Chem. Phys. 117 (20) (2002) 9478–9489.

[49] Y.-h. Song, L.-b. Zeng, Q. Zheng, Understanding the reinforcement and dissipation of natural rubber compounds filled with hybrid filler composed of carbon black and silica, Chin. J. Polym. Sci. 35 (11) (2017) 1436–1446.

[50] P. Dallas, A. Kelarakis, R. Sahore, F.J. DiSalvo, S. Livi, E.P. Giannelis, Self-suspended permanent magnetic FePt ferrofluids, J. Colloid Interface Sci. 407 (2013) 1–7.

[51] W. Hong, J. Lin, X. Tian, L. Wang, Viscoelasticity of nanosheet-filled polymer composites: three regimes in the enhancement of moduli, J. Phys. Chem. B XXXX (XXX) (2020).

[52] K. Kremer, G.S. Grest, Dynamics of entangled linear polymer melts, A molecular-dynamics simulation 92 (8) (1990) 5057–5086.

[53] C. Bennemann, W. Paul, J. Baschnagel, K. Binder, Investigating the Influence of Different Thermodynamic Paths on the Structural Relaxation in a Glass-Forming Polymer Melt, vol. 11, 1999, p. 2179, 10.

[54] H. Zhang, R. Ma, D. Luo, W. Xu, Y. Zhao, X. Zhao, Y. Gao, L.J.P. Zhang, Understanding the Cavitation and Crazing Behavior in the Polymer Nanocomposite by Tuning Shape and Size of Nanofiller 188, 2020, 122103.

[55] F.J. Galindo-Rosales, P. Moldenaers, J. Vermant, Assessment of the dispersion quality in polymer nanocomposites by rheological methods, Macromol. Mater. Eng. 296 (3-4) (2011) 331–340.

[56] J. Vermant, S. Ceccia, M. Dolgovskij, P. Maffettone, C. Macosko, Quantifying dispersion of layered nanocomposites via melt rheology, J. Rheol. 51 (3) (2007) 429–450.

[57] D.B. Genovese, Shear rheology of hard-sphere, dispersed, and aggregated suspensions, and filler-matrix composites, Adv. Colloid Interface Sci. 171 (2012) 1–16.

[58] W. Bauhofer, J.Z. Kovacs, A review and analysis of electrical percolation in carbon nanotube polymer composites, Compos. Sci. Technol. 69 (10) (2009) 1486–1498.

[59] J.C. Huang, Carbon black filled conducting polymers and polymer blends, Adv. Polym. Technol.: J. Polym. Process. Inst. 21 (4) (2002) 299–313.

[60] Y. Gao, F. Hu, Y. Wu, J. Liu, L. Zhang, Understanding the structural evolution under the oscillatory shear field to determine the viscoelastic behavior of nanorod filled polymer nanocomposites, Comput. Mater. Sci. 142 (2018) 192–199.

[61] V. Pryamitsyn, V. Ganesan, Origins of linear viscoelastic behavior of Polymer–nanoparticle composites, Macromolecules 39 (2) (2006) 844–856.

[62] G.D. Hattemer, G. Arya, Viscoelastic properties of polymer-grafted nanoparticle composites from molecular dynamics simulations, Macromolecules 48 (4) (2015) 1240–1255.

[63] W. Hong, J. Lin, X. Tian, L. Wang, Viscoelasticity of nanosheet-filled polymer composites: three regimes in the enhancement of moduli, J. Phys. Chem. B 124 (29) (2020) 6437–6447.

[64] T. Honek, B. Hausnerova, P. Saha, Relative viscosity models and their application to capillary flow data of highly filled hard-metal carbide powder compounds, Polym. Compos. 26 (1) (2005) 29–36.